Current-voltage characteristics of porous-silicon layers

D. B. Dimitrov
Institute of Solid State Physics, Bulgarian Academy of Sciences, Boulevard Tzarigradsko Chaussee 72, Sofia-1784, Bulgaria
(Received 31 May 1994; revised manuscript received 11 October 1994)

The current-voltage characteristics of porous-silicon structures are presented and discussed. Evidence is given that the forward and reverse currents show Schottky-junction-like behavior. Experimental measurements of reverse I-V curves at different ambient humidities demonstrate that the reverse current depends strongly on this parameter. The results are discussed in the light of generation-recombination processes in the porous-silicon depletion region. The presence of an inflection point in the reverse I-V curves is explained by the energy-band-gap difference between porous silicon and the crystalline silicon substrate.

Porous-silicon (PS) layers formed on monosilicon substrates by electrochemical etching have been known for many years. Most of the earlier work deals with the application of PS in different kinds of sensor devices.[1,2] Recently the interest of physicists in porous-silicon layers formed on monosilicon substrates has increased sharply, mainly because of the experimentally observed visible photoluminescence.[3–5] The origin of the photoluminescence (PL) has been discussed widely in scientific papers. Two different explanations are presented. The quantum confinement of electrons and holes in the crystalline silicon skeleton, proposed in Refs. 4–6, successfully explains the PL spectra of PS layers. An alternative theory proposes that the PL arises in different chemical species.[7–9] Most of the conclusions in both theories are based on the analysis of optical spectra and the composition of PS layers. Obviously additional investigations have to be carried out to understand the physical processes. Especially important is the analyses of electron and hole transport processes. In some recent works, the I-V curves of metal–porous-silicon–silicon (M-PS-S) junctions have been reported.[10–12,17] It is shown that M-PS junctions have Schottky-junction-like behavior. Despite such results, a detailed study of the I-V characteristics and a clarification of the transport mechanisms of the mobile carriers in porous Si is lacking. The unusually high reverse current is neither presented nor discussed.

In this paper, an analysis of the current-voltage characteristics of metal–porous silicon–monosilicon is presented. Special emphasis is given to the reverse [positive potential on the metal deposited on the PS layer (top of the structure)] current-voltage curves at different ambient humidities.

One of the major points in the formation of porous silicon is the thickness homogeneity of the layers. Usually this is ensured by preliminary p-type doping of the top of the wafers. In this case, because of the faster etching of the highly doped region, its depth determines the depth of the resulting PS layer. However, the doping itself may obscure the effect of porosity in subsequent measurements of the current along the direction of the electrochemical etching.

The substrates used in our experiments for fabrication of PS layers were 2-in., 50-Ω cm, p-type silicon wafers of (111) orientation. A good ohmic contact at the back side of the wafers was obtained by boron diffusion. An additional metal layer at the back side of the wafers was deposited by rf plasma sputtering. Wafers were anodized in a specially designed cell,[13] which allowed avoidance of contact between the back side metal and the electrolyte solution. For the electrochemical anodization, different solutions of hydrofluoric acid (HF), ethanol, and deionized water were used. A greater level of porosity was obtained by using a low concentration of HF (10%) and a high current density (150 mA/cm^2) (see Ref. 14). The good ohmic contact between the platinum ring and back side metal allows the establishment of a homogeneous porous-silicon layer on top of the wafer. The good ohmic contact at the back side, ensured by the boron diffusion and by the metal, is also of importance for subsequent measurements of current-voltage characteristics.

The current-voltage characteristics of metal–porous-silicon layer–silicon (M-PS-S) structures are measured using two different configurations, as shown in Fig. 1. The first type [Fig. 1(a)] is used to obtain the forward and reverse currents of M-PS-S structures. The second type [Fig. 1(b)] is used only to confirm the shape of the reverse current-voltage curves.

Typical I-V characteristics are shown in Fig. 2. The forward part of the measured I-V curve is very similar to a Schottky diode characteristic, and may be analyzed using the thermionic emission equation described by Sze:[15]

$$J_T = J_0 \exp(qV/nkT)[1-\exp(-qV/kT)] , \quad (1)$$

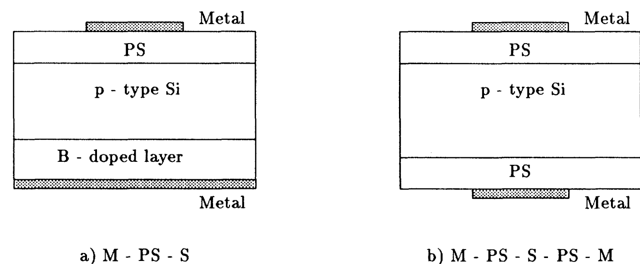

FIG. 1. Porous-silicon structures used for current-voltage measurements.

 ©1995 The American Physical Society

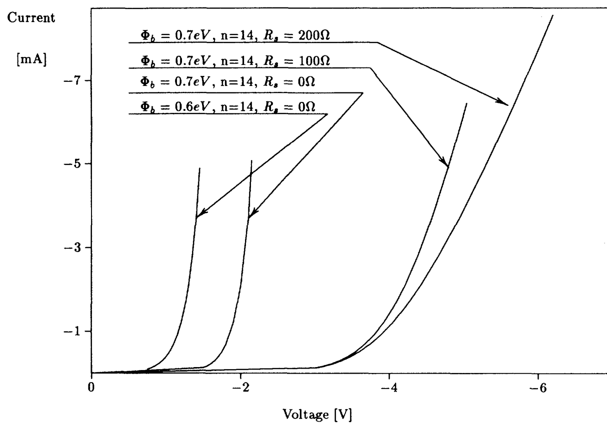

FIG. 2. Typical forward current-voltage characteristics of M-PS-S structures.

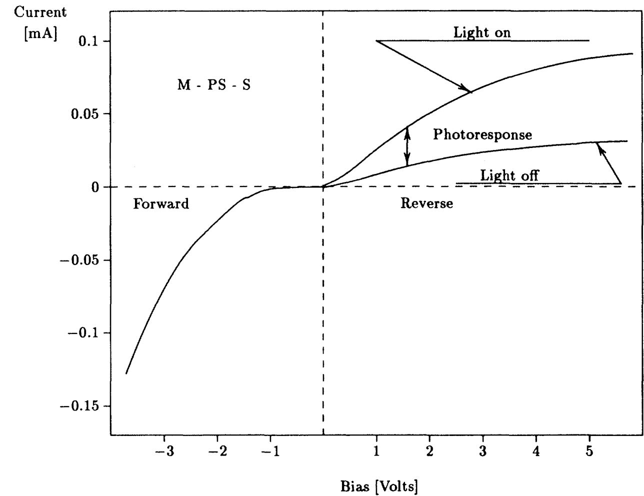

FIG. 3. Effect of daylight on current-voltage characteristics of M-PS-S structures.

where J_0 is the preexponential factor given by

$$J_0 = A^* T^2 \exp(-q\Phi_b/kT) . \quad (2)$$

A^* is the Richardson constant, and n is the ideality factor which accounts for any deviation of the measured forward current-voltage characteristics from the ideal behavior of a Schottky diode. The value of the ideality factor is interpreted in Ref. 16, where its relation to the interface states and to the possible thin insulator layer presented at the metal-semiconductor interface is given in the form

$$n = 1 - \frac{\delta\varepsilon_s}{W\varepsilon_i} + \frac{\delta q D_s}{\varepsilon_i} , \quad (3)$$

where D_s is the density of localized states at the M-PS boundary, W is the width of semiconductor space charge region, and ε_i and ε_s are the dielectric constants of the interphase and semiconductor regions, respectively. The I-V characteristics of the M-PS-S structures have been analyzed by fitting (1) to the measured forward curves in a way similar to that described in Ref. 17. For the fitting we take the value of $A = 32\ \text{cm}^{-2}\,\text{K}^{-2}$. The fitted parameters are the barrier height Φ_b and the ideality factor n. The obtained values for the latter parameter are close to the those given in Ref. 17. The value for n varies from sample to sample in the range 7.5–14, and is almost independent of the technological conditions for porous-silicon fabrication. However, to give physical meaning to n we need to know the value of ε for porous silicon. Assuming $\varepsilon = \varepsilon_{\text{Si}}$ and $\delta = 25$ Å (see Refs. 18 and 19) we may calculate the density of metal–porous-silicon interface states. For n varying between 7 and 14, the values of the corresponding densities of states vary between 5.17×10^{13} and $1.12 \times 10^{14}\ \text{cm}^{-2}\,\text{eV}^{-1}$. The simultaneous fit of Φ_b and n gives for the barrier height Φ_b at the metal–porous-silicon interface values of 0.65–0.7 eV. These values are very high in comparison to the barrier height at an Al p-type silicon Schottky junction.

The reverse current-voltage characteristics of M-PS-S structures are measured in the case of positive polarity of the metal electrode. They are very sensitive to the technological fabrication conditions for the samples. The dark current under reverse bias polarization in room air ambient (relative humidity was of the order of 30%) is shown in Fig. 3, where it is seen that the presence of room daylight strongly increases the reverse current. This is very similar to the sensitivity of a photodetector reported in Ref. 20, where it is found that the reverse current depends strongly on illumination. However, the shape of the reverse current-voltage curve indicates that the photogenerated carriers and associated light absorption takes place in the depletion region of the porous-silicon layer. Similar processes will be discussed further, analyzing the reverse current-voltage characteristics of PS in different ambient.

Under some circumstances, the reverse currents of the M-PS-S structures become sensitive to the ambient in the measuring cell. The samples prepared under conditions ensuring large pore size[14] show a strong dependence of the reverse current on the relative humidity (R_{H_2O}). The increase of the reverse current caused by increasing the R_{H_2O} from 1% to 90% is shown in Fig. 4 for two

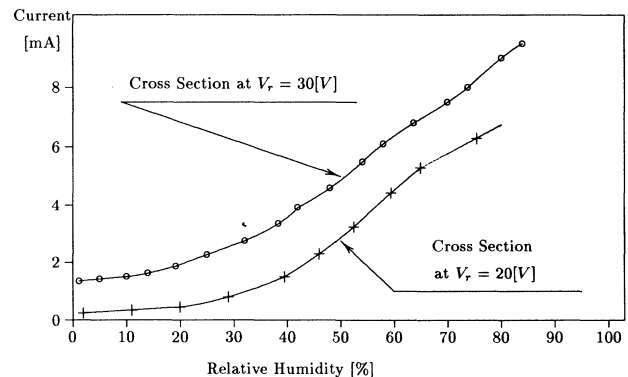

FIG. 4. Dependence of the reverse current of a M-PS-S structure on the relative humidity.

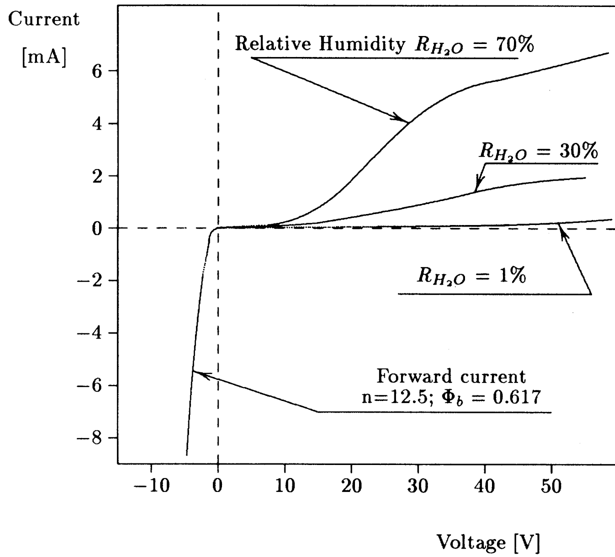

FIG. 5. Current-voltage characteristics of a *M*-PS-S structure at different values of ambient humidity.

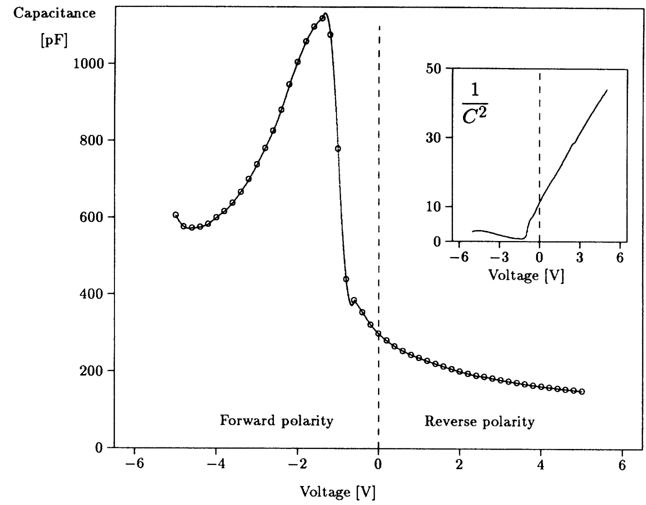

FIG. 6. Capacitance-voltage characteristics of *M*-PS-S structures. The inset shows $1/C^2$ dependence on reverse voltage.

different voltages. As can be seen from the figure, the two cross sections of the reverse current-voltage characteristics give only a parallel shift of the response. Hence we may conclude that the effect of humidity on the reverse current is not due to the moving of electrically charged particles in the frame of the *M*-PS-S structure. This fact may be explained by chemisorption of water in the porous silicon and subsequent physisorption on top of it. The water molecules of the first physisorbed layer are doubly hydrogen bonded to two surface hydroxyls and cannot move or rotate freely.[21]

The entire current-voltage characteristic of the *M*-PS-S structure for different ambient humidities is shown in Fig. 5. The forward current of the structure is insensitive to the humidity, and may be approximated again by the thermionic emission equation with $\Phi=0.617$ eV and $n=12.5$. The independence of the forward current on the humidity shows that the physical mechanism of humidity sensing differs from known humidity and hydrogen sensitive diodes,[22–24] where the sensitivity is based mainly on the change of the forward current or on the change of the impedance of the diode. In our case, although the reverse current of *M*-PS-S structures changes strongly depending on the humidity, the capacitance remains constant (for a given voltage) even in the case of a high humidity. The measured equivalent parallel capacitance of the structure (at 1 MHz) is shown in Fig. 6.

The strong dependence of the reverse current on the ambient humidity, and at the same time the absence of an effect of the humidity on the parallel equivalent capacitance C_p and on the forward current I_f, is a clear indication that the effect of humidity is connected to the recombination-generation current associated with the surface space-charge region of the Schottky junction formed between the metal electrode and the porous-silicon layer.[16] This current is observed even in the case of almost perfect PtSi-Si Schottky diodes.[25,26] The value depends only on the width of the depleted space-charge region W, and is described by

$$I_{\text{gen}}=q\frac{n_i W}{\tau_0} , \tag{4}$$

where n_i is the intrinsic carrier concentration of the semiconductor, and τ_0 is defined as the lifetime of the generated carriers and is connected to the density of the generation centers D_{st} ($\text{cm}^{-2}\,\text{eV}^{-1}$) and their effective capture cross section σ:

$$\tau_0=1/\sigma v_{\text{th}}\pi kTD_{\text{st}} , \tag{5}$$

where v_{th} is the thermal velocity of mobile carriers.

The dependence of the reverse current on the applied reverse voltage reflects the square-root dependence of the depletion layer width:

$$W=\left[\frac{\varepsilon_s\varepsilon_0}{2qN_A}\right]^{1/2}\left[\phi_b+V_r-\frac{2kT}{q}\right]^{1/2} , \tag{6}$$

where V_r is the voltage drop across the depletion region. The experimental results may be approximated by (4) if we accept that a part of the voltage applied to the *M*-PS-S structure drops over a parasitic resistance R_p, which is external to the depletion region. In this case the voltage drop over V_r reduces to $V_r=V_{\text{appl}}-V_p$, and expression (4) for the generated current can be rewritten in the form

$$I_{\text{gen}}=A\sqrt{[V_{\text{appl}}-V_{\text{bi}}]} , \tag{7}$$

where

$$A=q\frac{n_i}{\tau_0}\left[\frac{\varepsilon_s\varepsilon_0}{2qN_A}\right]^{1/2} \tag{8}$$

and

$$V_{\text{bi}}=V_p-\phi_b+\frac{2kT}{q} . \tag{9}$$

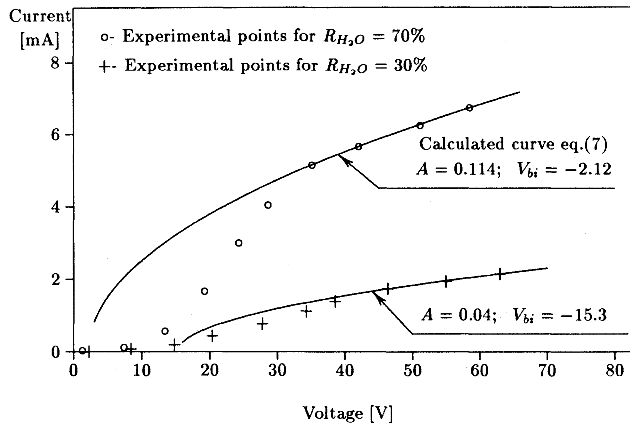

FIG. 7. Reverse current-voltage characteristics M-PS-S. The high-voltage part of the current is approximated by Eq. (7).

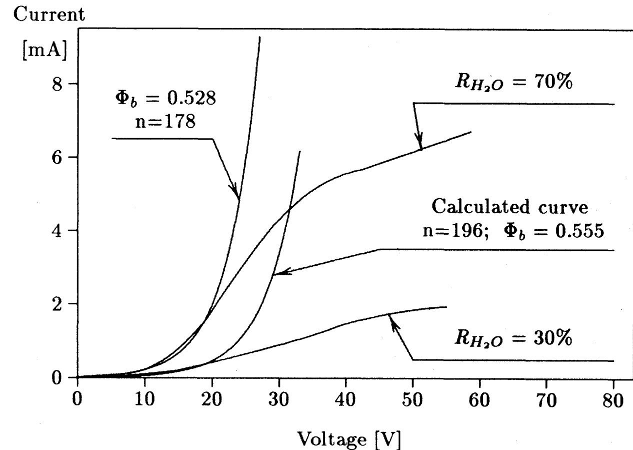

FIG. 8. Reverse current-voltage characteristics of M-PS-S. The limiting current in the low-voltage region is approximated by the thermionic emission equation.

The comparison between the current-voltage curves calculated by (7) and the experimental curves is presented in Fig. 7. As may be seen, correspondence between the calculated and experimentally measured current is good only for the high-voltage region of both curves. The shape of the experimental curve allows us to conclude that there is a current-limiting barrier only at low applied voltages. The presence of a second potential barrier at the porous-silicon–silicon interface may explain the presence of inflection in the experimentally observed reverse current-voltage characteristics. When the M-PS junction is biased in reverse polarity, the junction at the PS-S interface is biased in forward polarity.

If we accept that the current through the PS-S barrier obeys the thermionic emission equation (1), the current in the low-voltage region may be approximated again by fitting the ideality factor n and the barrier height. The curve calculated by (1) which best fits the experimental data is shown in Fig. 8. The ideality factor in this calculation is of the order of 130, which is too high in relation to the forward characteristics of a metal–porous-silicon junction. However, according to Eq. (3) this high value has to be expected because of the high density of interface states at the porous-silicon interface. Assuming again that an insulator layer of the order of 25 Å is present at the PS-S interface, the high ideality factor determined using (3) may be attributed to an effective density of interface states of the order of 1.11×10^{15} $cm^{-2}\,eV^{-1}$.

These considerations imply that the PS-S junction may be treated as a heterojunction between two semiconductors with different forbidden gaps. According to the existing theory of the isotype heterojunction presented by Milnes and Feucht,[28] it may be expected that the forward current (PS negative) also will saturate at some value. Because of the early breakdown, however, the saturation current is difficult to determine experimentally. Actually our experimental measurements show that when the forward current reaches a value of 100–150 mA/cm^2 a bright visible electroluminescence (EL) may be observed when the metal is semitransparent. The intensity of this light depends on the current density, and has been interpreted by Koshida and Korama[11] and Wang and Zheng[29] as resulting from electron and hole injection from metal electrodes and p-type Si substrates into the PS. The observed electroluminescence is not dependent on ambient humidity. The fast change of the ambient humidity from 30% to 70% has no effect on the emitted light. Having in mind that the high ambient humidity implies a high density of states in the PS, it has to be concluded that the radiative process of EL takes place inside the silicon columns which form the PS but not at the micropore walls inside the PS layer. The variation of density of states has no effect on the EL spectra, and only the size of the silicon columns determines the light emission. However, detailed study of EL in different gases has to be carried out to increase the duration of light emission.

In summary, we have presented an analysis of $I-V$ characteristics of metal–porous-silicon structures for different ambient humidity conditions. It is shown that the forward current and the depletion capacitance are independent of ambient humidity. The reverse current (metal positive) depends strongly on ambient humidity. The analysis of the reverse I-V curves shows that current generation in the depletion region takes place due to the presence of generation centers in the depleted porous-silicon region. The density of these centers depends on the relative ambient humidity during the measurements. The exact kinetics of the incorporation of the generation centers in the porous-silicon layer is not discussed here, and is presented elsewhere.[27] The changes introduced by the different ambient humidities are determined by the porosity of the layers. The shapes of the reverse I-V curves indicate the presence of an energy-band-gap discontinuity at the porous-silicon–silicon boundary. It is proposed that the band-gap discontinuity arises from the energy-band-gap difference between the porous-silicon layer and the monosilicon substrate.

This work has been supported by Bulgarian Ministry of Science and Education under Contract No. Φ322. The author is strongly indebted to Professor J. Marshal for helpful discussions.

[1]R. Iscoff, Semicond. Int. **8**, 30 (1991).
[2]M. Yamana and N. Kashiwazaki *et al.*, J. Electrochem. Soc. **137**, 2925 (1990).
[3]R. Fathauer, T. George, A. Ksendzov, and R. Vasquez, Appl. Phys. Lett. **60**, 995 (1992).
[4]S. Shih, K. Jung, and R. Quan, Appl. Phys. Lett. **62**, 467 (1993).
[5]S. Gardelis, J. Rimmer, P. Dawson, and B. Hamilton, Appl. Phys. Lett. **59**, 2118 (1991).
[6]L. Canham, Appl. Phys. Lett. **57**, 1046 (1990).
[7]K. J. Nash, L. T. Canham, and A. G. Cullis, Europhys. News **23**, 183 (1992).
[8]S. Brandt *et al.*, Solid State Commun. **81**, 307 (1992).
[9]M. Stutzmann, M. Brandt, M. Rosenbauer, J. Weber, and H. Fuchs, Phys. Rev. B **47**, 4806 (1993).
[10]R. Anderson, R. Muller, and C. W. Tobias, J. Electrochem. **138**, 3406 (1991).
[11]N. Koshida and Y. Korama, Appl. Phys. Lett. **60**, 347 (1992).
[12]F. Namaver, H. Maruska, and N. Kalkoran, Appl. Phys. Lett. **60**, 2514 (1994).
[13]G. Beshkov, D. Dimitrov, and M. Kamenova, Electron. Electrotechnics **10**, 43 (1993).
[14]R. Herino, G. Bomchil, K. Barla, and C. Bertrand, J. Electrochem. Soc. **134**, 1994 (1987).
[15]S. M. Sze, *Physics of Semiconductor Devices,* 2nd ed. (Wiley, New York, 1980).
[16]A. Grove and D. Fitzgerald, Solid State Electron. **9**, 783 (1966).
[17]H. Maruska, F. Namavar, and N. Kalkhoran, Appl. Phys. Lett. **61**, 11338 (1992).
[18]H. Card and E. Rhoderick, J. Phys. D **4**, 1589 (1971).
[19]H. C. Card, Solid State Commun. **14**, 1011 (1974).
[20]J. Zheng, K. Liau, and W. Shen *et al.*, Appl. Phys. Lett. **61**, 2514 (1992).
[21]N. Yamazoe and Y. Shimizu, Sensors Actuators **10**, 379 (1986).
[22]H. Kobayashi, K. Kishimoto, Y. Nakamoto, and H. Tsubomura, Sensors Actuators B **13-14**, 125 (1993).
[23]Sh. Nakagomi and T. Yamamoto, Sensors Actuators B **13**, 617 (1993).
[24]Y. Ushio, M. Miyayama, and H. Yanagida, Sensor Actuators B **12**, 135 (1993).
[25]M. Wittmer, Phys. Rev. B **42**, 5249 (1990).
[26]M. Wittmer, Phys. Rev. B **43**, 4385 (1991).
[27]D. B. Dimitrov *et al.*, J. Phys. (to be published).
[28]A. G. Milnes and D. L. Feucht, *Heterojunctions and Metal Semiconductor Junctions* (Academic, New York, 1972), p. 94.
[29]J. Wang and Fu-Long Zhang *et al.*, J. Appl. Phys. **75**, 1070 (1994).